

Laser Surface Hardening of the Carbon Enriched Duplex Stainless

K. Yildizli, T. Kayalarli, C. Dengiz, H. Cep

ABSTRACT

In this study, DIN No.1.4462 standard sheet was chosen as duplex stainless steel sample. For the purpose of carbon bearing to subsurface, graphite powder was coated on the sheet sample surface by spraying. A CO₂ laser source integrated manipulator robot was used for surface modification treatment. The laser beam was linearly travelled on the coated steel surface at different travelling speeds, followed by quenching in air. In conclusion, the Ni equivalent arose with increase in the carbon content on surface. Much lower laser travelling speeds resulted in the resolidificated surface. The cross sectional microstructure was scanned with the biaxial EDX mapping and surface hardness measurements after laser applications. The high laser heat input hardly distorted dual phases just beneath the dual phase microstructure and limited alloyed with carbon. Surface melting and quenching render crystallographic martensite and few carbide transformations from austenite phases. For these reasons, the sheet surface can harden despite overheating, sheet distortion, unreasonable carbon and oxygen-rich impurities on the laser modified section. This hardening methodology can delay the wear and deformation of local mold surfaces, and new surfactants, e.g. spray, paste and cream, can be developed for fast carbon enrichment of stainless steels sheets.

1 INTRODUCTION

Laser beam is a direct surface heater and a tool for surface engineering [1]. In fact, the applied energy can be focused on precisely on the surface only where it is needed [2]. Laser surface hardening are applied on Fe-C and Fe-Cr-C alloys and in Fe-Cr-Mn-C alloys [3], the applications resulted in sometimes positive or negative effects like dissolved pearlite colonies resulting from incomplete austenisation and limited austenisation depth distance from surface. Steels and cast irons are preferred for laser hardening. In this process, a thin layer of ferrous surface is rapidly heated well into austenitizing temperature by laser heating and subsequently quenching in air [4]. Previous research studies were recently reviewed by Majumdar and Manna [5]. Hypo-eutectic steels with low carbon [6] e.g, SAE 1010 [7], SAE

1018 [8] SAE 5135 [9], AISI 4140 [10], and H13 [11] and tempered 4340 [12] steel workpieces were hardened with low or high power laser beam [13], from a few watts and 20 kW, as well as the stainless steels [14].

The austenitic stainless steels are not appropriate for martensite transformation because of stable full austenitic phase during rapid quenching, and powder metal (PM) 304 either [15]. Therefore, commonly AISI 304, AISI 316 and 316L cannot be systematically hardened expect for submicron or micro-scaled hardening depths [8,16]. The basic reason is austenite stability and insufficient free carbon atoms need for martensite transformation. After remelting and resolidification, unbalanced Cr and Ni wt% is also problematic in terms of microsegregation, knife edge and stress-corrosion cracking risk at grain boundaries. However, laser alloying of AISI 304 was made with microstructure dispersion of the added materials, i.e, WC, TiN and TiB₂, subsequently cooled at a very fast rate due to self-quenching to possible iron-carbide (cementite) and martensite transformation [17]. The laser surface hardening can be applied to localized areas on large metal surfaces i.e. sheet metals.

Duplex stainless steels (DSS) cannot be adequately hardened by post heat treatments because they contain insufficient free carbon content, stable austenite and ferrite phases. The dual phase 1.4462 sheet is a good example for applying a new laser surface modification and subsequently hardening in air. There are few data for duplex stainless steels, not in a sheet form. Effects of laser surface alloying with SiC powder on microstructural changes and properties of vacuum sintered austenitic X2CrNiMo17-12-2, ferritic X6Cr13 and duplex X2CrNiMo22-8-2 stainless steel were investigated [15]. Pitting and intergranular corrosion resistance of duplex stainless steels were improved by means of dispersion of WC particles embedded in the cast duplex stainless steel matrix [18]. Kwok et al. [19] reported an improvement in the intergranular corrosion resistance of two aged DSS plates, UNS S31803 and S32950, after surface melting with a 1kW Nd: YAG laser. Capello et al. [20] realized elimination of undesired delta ferrite in weld zone of 22Cr-5Ni-3Mo (UNS S32205) DSS with CO₂ laser. However, future of submicron applications on the stainless steel applications

looks like limited. Carbon enrichment is more applicable for sheet metal surfaces than dispersion alloying and submicron methods. We need to find deeper hardening strategy for stainless steels.

1.1 MATERIAL AND METHOD

The 3 mm thick DIN No.1.4462 standard sheet was chosen as duplex stainless steel sample. For the purpose of carbon bearing to subsurface, graphite powder was previously coated on the sheet sample surface by spraying. A 3 kW CO₂ laser source integrated manipulator robot was used for surface modification. The laser beam was linearly travelled on the graphite coated steel surface at different travelling speeds at 600 W beam energy, following by quenching in air for crystallographic martensite transformation. DSS etchant was 30 ml HCl+15 ml HNO₃+5 ml HF for metallographic examination.

Element	C	Si	Mn	P	S	Cr	Ni	Mo	N	Cu	Ti	Ce
wt%	0.016	0.41	1.34	0.022	0.001	22.22	5.71	3.12	0.169	0.21	0.005	0.015

Tab.1 Chemical composition of DIN Material No: 1.4462 Duplex stainless steel

2 CARBON ENRICHMENT ON SHEET

In this study, two different carbon bearing agents, the milled graphite powder and CH₄ gas, were used. The carbon enrichment applications were explained at below

The initial free C, Cr and Ni equivalents of 1.4462 sheet were calculated on Schaeffler-DeLong diagram and the surface chemical composition was modified with two different carbon enrichment applications in order that the surface microstructure can be shifted toward martensite phase fields on the diagram.

2.1 GRAPHITE POWDER SPRAYING

The graphite powder was sprayed on the sheet workpiece, as shown in Fig.1. The sheet surface was coated with graphite layers two times before the laser beam sending on the sheet surface.

This can be possible with using carbon bearing agents, graphite powder or carbon bearing solid or gases near future.

This study describes how to use laser beam scanning strategy with robotic integration after carbon enrichments on DSS sheet

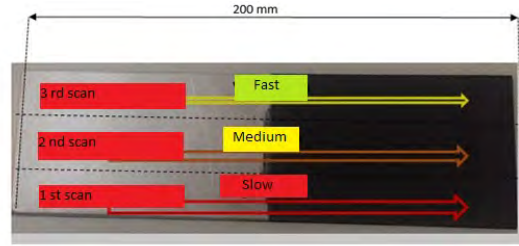


Fig. 1 The 1.4462 sheet surface coated half by half. (Uncoated / coated sites)

2.2 GAS CARBURISING (CEMENTATION)

Gas cementation was applied in a furnace with CH₄ atmosphere at 950°. For the 1 mm carbon diffusion depth from the sheet surface cementation duration was calculated as 21 hours according to Fick's second law.

2.3 CHROMIUM NICKEL AND CARBON EQUIVALENTS

The carbon, chromium and nickel equivalents were calculated by Equations 1,2 and 3 respectively. Using the equations, it is need to determine the equivalents of the C, Cr and Ni elements in wt. The chromium equivalent is given in (1):

$$Cr_{eqv} = Cr\% + Mo\% + 1.5Si\% + 0.5Nb\%$$

$$Cr_{es} = 22.22 + 3.12 + 1.5 \times 0.41 + 0 \rightarrow Cr_{eqv} = 22.955 \quad (1)$$

$$Ni_{eqv} = Ni\% + 30\%C + 0.5Mn\%$$

$$Ni_{eqv} = 5.71 + 30 \times 0.016 + 0.5 \times 1.34 \rightarrow Ni_{eqv} = 6.86 \quad (2)$$

$$C_{eqv} = C\% + \frac{Mn\%}{6} + \frac{Cr\% + Mo\%}{5} + \frac{Cu\% + Ni\%}{15} \quad (3)$$

Substitution in (3)

$$C_{eqv} = 0,016 + \frac{1,34}{6} + \frac{22.22+3.12}{5} + \frac{0,21+5,71}{15} \rightarrow C_{es} = 5.702$$

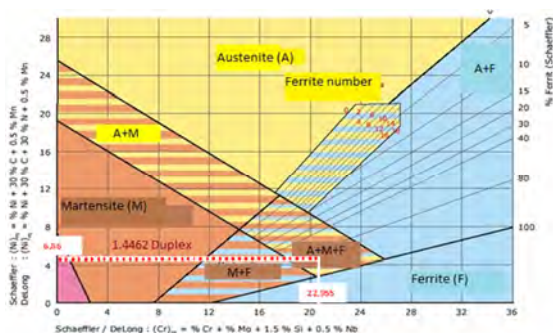


Fig. 2 Position of the DIN Material No: 1.4462 on Schaeffler-DeLong Diagram

Ni equivalent arose with increase in the carbon content on surface. On the diagram in Fig.2, the % coefficient of carbon element is 30 and therefore, It is noticed that vertical position of the 1.4462 sheet material can shift to backward and upward after carbon enrichment with the laser intergration.

2.4 LASER HARDENING

Surface hardening was performed by a 3 kW laser beam integrated robot manipulator, ALOtec Dresden, GmbH, in an industrial company, RUKOSEN, Istanbul. The laser beam travelling speeds were defined slow, medium and fast. The laser scan distance is almost 200 mm and the scanned width is 1.5 cm for each every scan.

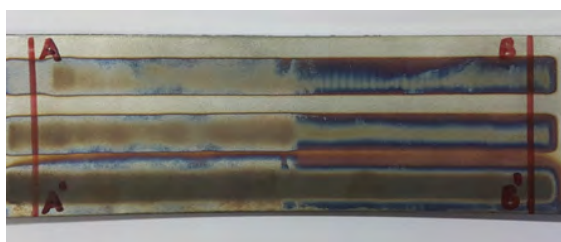


Fig. 3 Laser hardened surface at three different travelling speeds (Sections AA' and BB' refer to as the extracted sample positions from the uncoated and the graphite coated surface regions after laser application, respectively)



Fig. 4 Laser hardened sheet surface after gas cementation

3 RESULTS

3.1 ESTIMATED SURFACE TEMPERATURE

Analytic equation describing the steady state and three dimensional heat flow in a moving semi infinite workpiece model subjected to a stationary square (or rectangular) heat source was first derived by Jaeger 1943 [1,4]. We used a welding heat source model in [21], considering as if laser beam was welding electrode. The assumptions made were equivalent to (1) no surface heat loss due to convection or radiation (2) constant thermal properties and (3) constant surface absorptivity.

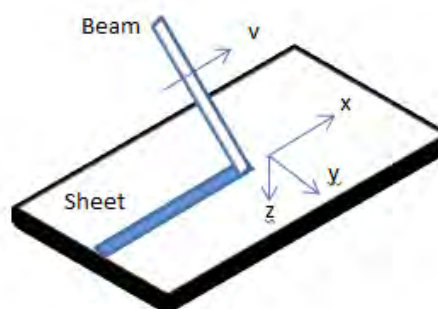


Fig. 5 Moving heat source trajectory on sheet for laser beam (adapted from [21])

Temperature distribution of beam region can be estimated in laser hardening treatment. The generated surface temperature about heat source was calculated by following assumptions, material parameters and measurements on the treated sheet.

Hence a laser beam is assumed as welding electrode with a spherical tip. The coordinate axes for the beam are defined as x and y on sheet surface and z in depth.

Beam radius : $r = 1 \text{ mm} = 10^{-3} \text{ meter}$

Sheet density : $\gamma = 7.955 \text{ milligram per cubic meter}$

Thermal Conductivity: $k = 15,5 \text{ Watts per meter.Kelvin}$

Specific heat capacity: $C_p = 510$

Joule/kg. Kelvin

Hence thermal diffusivity coefficient : α

$$\alpha = \frac{k}{\gamma \cdot c} = 0,058 \text{ square meters per second}$$

Power (P) = 0,2 kWatt and b: Conversion factor: 0.24 (steel welding application[1].)

$$q = 0,24 \cdot V \cdot I = 0,24 \times 200 \\ = 48 \text{ calories per second}$$

For beam travelling speed (v);

$v = 1 \text{ millimeter per second}$; the laser treated zone width (x) was measured as the almost 15 millimeters

$$x_1 = \frac{15 \text{ mm}}{2} = 7,5 \text{ mm}$$

$$T = \frac{q}{2 \cdot \pi \cdot k \cdot r} e^{-\frac{\theta(x+r)}{2\alpha}}$$

$$\rightarrow T_1 = \frac{48 \frac{\text{cal}}{\text{s}} \cdot 4,18 \frac{\text{j}}{\text{cal}}}{2 \cdot \pi \cdot 15,5 \frac{\text{W}}{\text{mK}} \cdot 10^{-3} \text{m}} e^{-\frac{10^{-3}(7,5+1)10^{-3} \text{m}}{2 \cdot 0,058 \frac{\text{m}^2}{\text{s}}}}$$

$$= 2060,03 \text{ K} = 1,787,03^\circ \text{C}$$

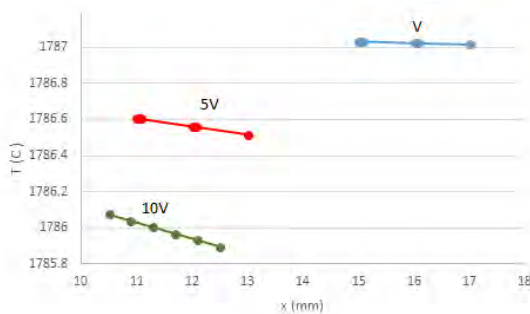


Fig. 6 Estimated temperature distribution about laser beam source

Fig.6 shows estimated temperature distribution about x direction during the laser application. If the beam travelling speeds increases up ten times (10xV), melting zone is the narrowest. Theoretical calculated temperature is about 1750°C which is enough for melting steel. However, using thermal camera average measured surface temperature was almost 1250°C . The significant difference between calculated and experimental temperature data can be reduced by changing, the conversion

factor, laser power (P) and efficiency in industrial applications.

3.1.1 Biaxial chemical mapping

In order performing EDX mapping, JEOL 7001F Field Emission (FE) Scanning Electron Microscope (SEM) was used with an EDX attachment with the 80 mm^2 X-MAX detector. An etched microstructure image of 1.4462 sheet sample is seen in Fig .7, the lower phase is austenite and upper phase is ferrite [22]. An un-uniform carbon-rich layer lies on dual phases of the surface. In Fig. 8, the detected element maps were given in queue. The map images identify biaxial distribution of the different elements of the carbon enriched sheet microstructure. It is noticed that the carbon and oxygen maps are subordinate to each other. The laser beam hardly affects on ferrite and austenite phases. A fully melted zone on the sheet is not observed. Although strong carbide evidence was not found expect for deposited carbon-rich surface layer. After the laser applications,,the surface hardness increased up 35-45 HRC according to the hardness measurements. This increase in the hardness can be related with remarkable martensitic transformation and together dislocations (not viewed here), or residual stress in the dual phase microstructure, not carbides. It is considered that sprayed carbon layer could be flammable and evaporated when the laser beam was sent on the surface. Graphite impurities and voids on the carbon-rich layer were observed related with dissolved graphite and CO combination of intensive Carbon and Oxygen atom [4]. These findings are negative indicators for laser beam, depicting insufficient left on dual phase microstructure.

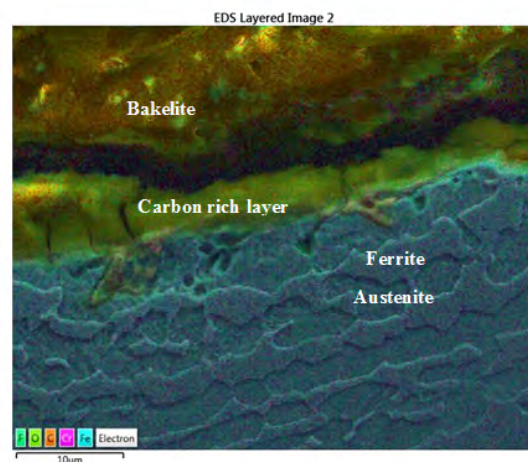


Fig. 7 Subsurface microstructure of the carbon-rich sheet sample

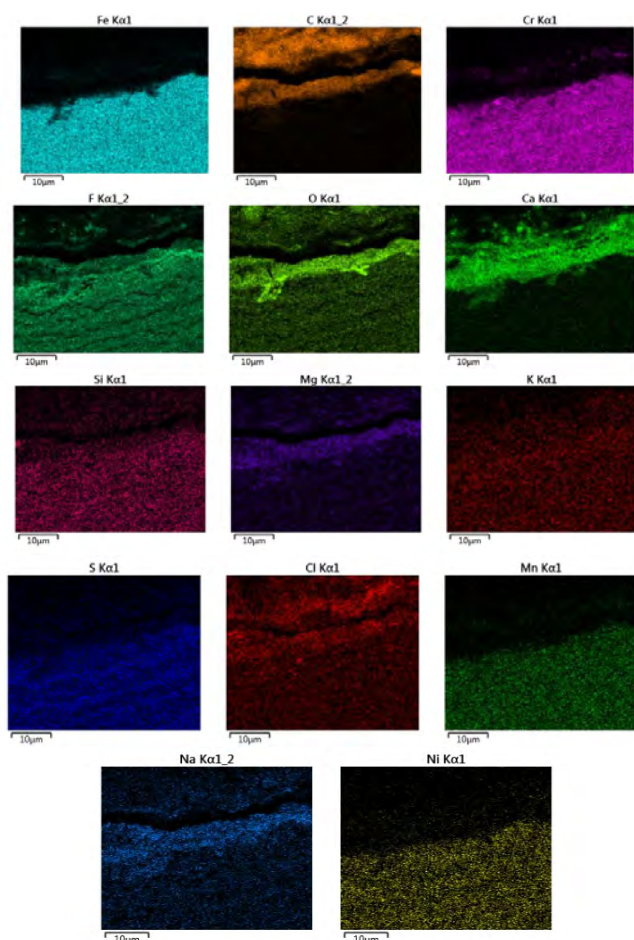


Fig. 8 Elements maps of powder sprayed sheet surface (transverse sample section)

3.1.2 Chemical composition after laser treatment

Chemical composition of the laser treated surface is listed in Table 2. In particular, the content of C, Cr, Ni, Mo and Mn remarkably increased and so C, Cr and Ni equivalents are calculated from Table 2 for determining position of carbon enrichment treatment on the Schaeffler-Delong diagram.

Elements (%wt.)	C	Cr	O	F	Ca	Ni	Mo	Cl	Mn	Mg	Na
After laser	32	13	5.7	4.5	3.4	3	1.7	1.1	0.1	0.1	0.07
Before laser	0.016	22.22				5.71	3.12		1.34		

Tab. 2 Chemical elements after carbon enrichment.

4 DISCUSSION

Carbon diffusion from the surface take times. For a one millimeter diffusion depth, heating duration is almost 21 hours. Overheating resulted in thermal distortion of DSS sheet metal. The sheet metal hardness increased up 35-45 HRC. Local and high laser heat input led to less thermal distortion of sheet. Prior to laser heating, thickness of sprayed graphite layer was bigger than the approximately 10 microns carbon-rich layer on the DSS confirmed by EDX mapping. This marks to a mass loss relative to initial graphite coating layer. The reason of thickness reduction can be resulting from carbon burning in the sprayed graphite coating since carbon coating is flammable. The C and O maps have similar layer geometry. It is noticed that these maps can be evidence for carbon flame because flame is occurred if oxygen present. In case of a part of carbon layer burning by laser beam, interstitial carbon atoms penetrates distance from surface by way of plasma mechanisms, ionisation and implantation (not now strong evidence). It is also observed that the carbon-rich layer involves porosity and vertical cracks based on the visual images in this study. EDX analyses confirmed carbon enrichment on DSS surface, Unexpectedly, no carbides were found. Furthermore, The 32 wt%.carbon content measurement was inconsistent for virgin DSS and laser treated DSS sheets because carbon dissolubility in f.c.c and b.c.c iron phase is limited [22]. It doesn't exceed 2.07 % in austenite phase in Fe-C alloys.

5 CONCLUSIONS

This paper presents carbon enrichment trials for the DSS sheet. Surface temperature prediction and the subsurface microstructure are discussed after laser surface hardening. In particular, two different carbon enrichment strategies are considered:

Carbon-rich layer was produced on DSS sheet. High power laser beam cannot be alloyed with free carbon.

Carbon enrichment treatments can be systematically defined on Schaeffler-Delong diagram for stainless steels.

Temperature distribution near the beam can be estimated by weld source model in this study. This basic model can be benefit for avoiding the overheating temperature in austenitisation. The workpiece and the scanning strategy

make it possible to control the hardening of the sheet metal.

6 ACKNOWLEDGMENTS

This study partly contains some laser hardening trials and preliminary results under project contract no: 0754.STZ.2014. The use of the facilities of Karadeniz İleri Teknoloji Araştırma ve Uygulama Merkezi (KITAM) at Ondokuz Mayıs University and SAMPAM Automotive R&D Center, SAMSUN are acknowledged. The authors thank the staffs and managers for applications with the laser hardening robot of RUKOSEN, Miltas Ltd.Sti. Tuzla ISTANBUL, TURKIYE

7 REFERENCES

- [1] Steen, W.M.: Laser Surface Treatment, Laser Material Processing, Chapter6, Springer-Verlag, London, 1991.
- [2] Mai, T.A.; Lim, G.C.: Micromelting effect and its effect on surface topography and properties in laser polishing of stainless steel, Journal of Laser Applications, 22(16), December 2004.
- [3] Bradley, R.; Sooho, J.; Kim.: Laser transformation hardening of Iron-carbon, Iron-carbon-chromium steels, Metallurgical Transactions A, Vol .19A, August 1988, p.2013.
- [4] Majumdar, J.: Laser heat treatment, State of the art, Journal of Metal, p.18., May 1983.
- [5] Majumdar, J.D.; Manna, I.: Laser material processing, International Materials Reviews, Taylor&Francis, Vol: 56,: 5-6, pp. 341-388. Institute of Materials, Minerals, and Mining, ASM International, 12 November 2013.
- [6] Orazi, L.; Fortunato, A.; Cuccolini, G.; Tani, G.: An efficient model for laser model hardening of hypo-eutectic steels, Applied surface science, 256, pp.1913-1919, 2010.
- [7] Chu, J.P.; Rigsbee, J.M.; Banas, G.; Elsayed-Ali, H.E.: Laser shock processing effects on surface microstructure and mechanical properties of low carbon steel. Materials Science and Engineering A260, pp.260-288, 1999.
- [8] Kou, S.; Sun D.K.; Le Y.P.: A fundamental study of laser transformation hardening, Metallurgical Transactions A, vol. 14A 247, pp. 643-, April 1983.
- [9] Selvan, J.S.; Subramanian, K.; Nath, A.K.: Effect of laser surface hardening on En 18 (AISI5135) steel, Journal of Materials Processing Technology, 91,pp.29-36,1999.
- [10] Miokovic, T.; Schulze, V.; Volringer, O.; Lohe, D.: Cycle temperature changes on the microstructure of AISI 4140 after laser surface hardening, Acta Materialia, Vol: 55, pp. 589-599, 22 August, 2007.
- [11] Lee, J-H.; Jang, J-H.; Joo, B-D.; Son, Y-M.; Moon, Y-H.: Laser surface hardening of H13 tool steel, Transactions of Nonferrous Metals Society of China, Vol: 19, pp.917-920, 10 March 2009.
- [12] Shiue, R.K.; Chen, C.: Laser transformation hardening of tempered 4340 steel, Metallurgical Transactions A, Vol 23A, p163, January 1992.
- [13] Keneddy, E.; Byrne, G.; Collins, D.N.: A review of the use of high power diode lasers in surface hardening, Journal of Materials Processing Technology, Vol: 155-156, pp.1855-1860, 2004.
- [14] Yang, L.J.; Tang, J.; Wang, M.L.; Wang, Y.; Chen, Y.B.: Surface characteristics of stainless steel sheet after pulsed laser forming, Applied Surface Science Vol: 256, 23, 15 September 2010.
- [15] Brytan, Z.; Dobrzański, L.A.; Pakieła, W.: Laser surface alloying of sintered stainless steel with SiC powder. Journal of Achievements in Materials and Manufacturing Engineering,47(1), pp.42-56. 2011.
- [16] Laroudie, F; Tassin, C; Pons, M.: Hardening of 316 L austenitic stainless steel by laser surface alloying, Journal of Materials Science 30, pp.3652-3657,1995.
- [17] Levkovici, S.M.; Levkovici, D.T.; Munteanu, V.; Paraschiv, M.M.; Preda.: Laser surface hardening of austenitic stainless steels, A, Journal of Materials Engineering and Performance, ASM International, pp. 536-540, 9(5) 2000.
- [18] Do Nascimento, A.M.; Ocelik, V.; Lerardi, M.C.F.; De Hosson, J.Th.M.: Microstructure of reaction zone in WCp/duplex stainless steels matrix composites processing by laser melt injection, Surface and Coatings Technology, Vol 202(10), pp.2113-2120, 15 April 2008.

[19] Kwok, C.T.; Lo, K.H.; Chan, W.K.; Cheng, F.T.; Man, H.C.: Effect of laser surface melting on intergranular corrosion behavior of aged austenitic and duplex stainless steels, Corrosion Science, 53, pp.1581-1591. 28 January 2011.

[20] Capello, E.; Chiarello, P.; Previtali, B.; Vedani, M.: Materials Science and Engineering A, Vol: A351, pp.334-343, 2003.

[21] Baggerud, A.: Welding Metallurgy, 1sted., Translated to Turkish Edition by Selahattin Anik and Kutsal Tulbentci: Istanbul, p.103., 1966.

[22] Yildizli, K.: Investigation of microstructure and toughness properties of austenitic and duplex stainless steels weldments under cryonic conditions, Materials and Design, 77, pp.83-94,15, July 2015.

Author: Yildizli, Kemal
University: Ondokuz Mayıs Univ.
Department: Dept. of Mechanical Eng.
E-Mail: kyildizli@omu.edu.tr
